Supplementary Information

# Thermal Dehydration of D-Glucose Monohydrate in Solid and Liquid States

Kazuki Kato, Masami Hara, and Nobuyoshi Koga*

Department of Science Education, Division of Educational Sciences, Graduate School of Humanities and Social Sciences, Hiroshima University, 1-1-1 Kagamiyama, Higashi-Hiroshima 739-8524, Japan.

## Contents



* Corresponding author: e-mail: nkoga@hiroshima-u.ac.jp

## S1. Sample characterization

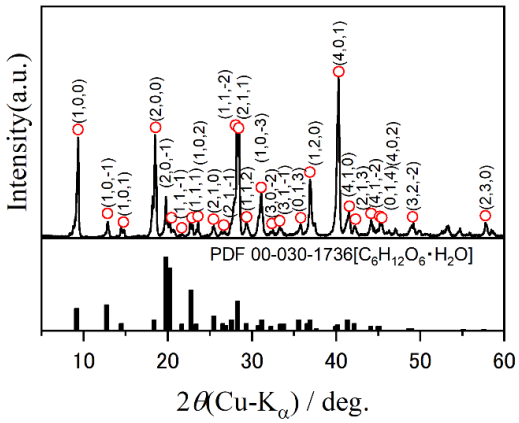


**Figure S1.** XRD pattern of the sample.

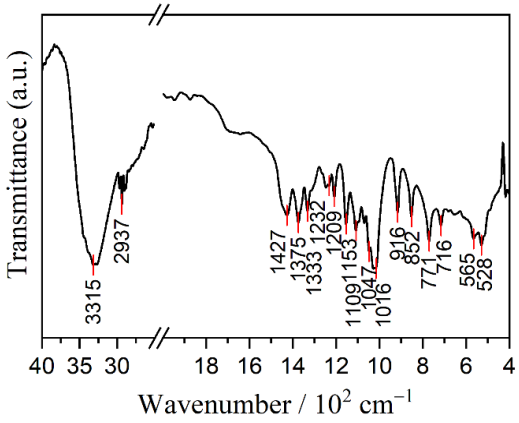


**Figure S2.** FTIR spectrum of the sample.

**Table S1.** Attributions of the IR absorption peaks

| Peak position /cm$^{-1}$ | Vibration mode |
|---|---|
| 2850–3600 | $\nu$OH, $\nu_s$CH and $\nu_{as}$CH |
| 1427 | $\delta CH_2 + \delta OCH + \delta CCH$ |
| 1375 | $\delta OCH + \delta COH + \delta CCH$ |
| 1333 | $\delta CCH + \delta OCH$ |
| 1232 | $\delta CH + \delta OH$ |
| 1209 | $\delta CH + \delta OH$ in plane |
| 1153 | $\delta CO + \nu CC$ |
| 1109, 1016 | $\nu CO$ |
| 916 | $\nu CO + \nu CCH + \nu_{as}$ ring of pyranose |
| 600–1500 | $\nu CO$, $\nu CC$ |

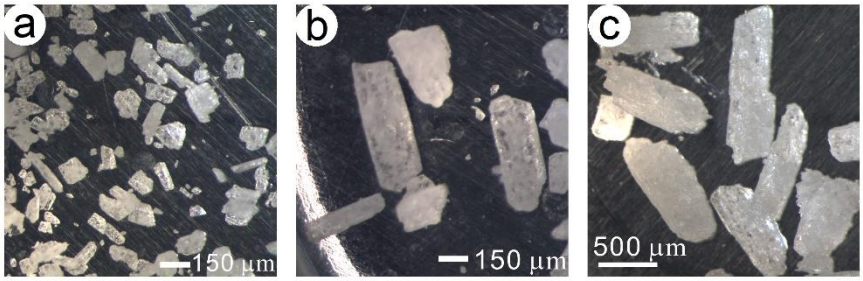


**Figure S3.** Sample particles of different particle size fractions: (a) 90–150. (b) 150–300, and (c) 300-500 µm.

## S2. Experimental setup for TG–DTA measurements

The simultaneous TG–DTA instrument (DTG60, Shimadzu) is composed of a vertically arranged differential microbalance and a furnace. Prior to TG–DTA measurements, the instrument was calibrated with regard to the measured temperature and mass change, using standard methods. The temperature calibration was performed with reference to the onset temperature of the endothermic DTA peaks for the melting of pure metals (Ga, In, Sn, Pb, Zn, Al, and Ag, ≥ 99.99% purity, Nilaco), observed during heating at a $\beta$ of 5 K min$^{-1}$ in a stream of dry $N_2$ ($q_v$ = 100 cm$^3$ min$^{-1}$), by comparing with the literature value of the melting point. The mass change value was initially calibrated by the addition/removal of the standard weight (2.00 mg) in an open atmosphere. Subsequently, the mass loss values for the three thermal dehydration/decomposition steps of $CaC_2O_4 \cdot H_2O$ ($m_0$ = 5.0 mg, ≥99.9985%, Alfa Aesar) were observed during linearly heating at a $\beta$ of 5 K min$^{-1}$ in a stream of dry $N_2$ ($q_v$ = 100 cm$^3$ min$^{-1}$). For the TG–DTA measurements, 5.00 mg of $Al_2O_3$ weighed in a Pt pan (diameter: 6 mm; depth: 2.5 mm) was used as

the reference for DTA and counter-balance for TG.

The humidity-controlled TG–DTA instrument is composed of a horizontally arranged differential microbalance with a furnace (TG-8122, Thermoplus Evo2 system, Rigaku) and a humidity controller (me-40DP-2PHW, Micro Equipment Co.). The gas flow route in the instrument, including the transfer tube between the humidity controller and anterior chamber, anterior chamber of the reaction tube, and reaction tube, was heated at a temperature higher than the dew point of the introduced $N_2$–$H_2O$ mixed gas to avoid the possible condensation of the water vapor. A mixed $N_2$–$H_2O$ gas with a controlled $p(H_2O)$ was introduced into the reaction tube via the anterior chamber at $q_v$ = 200 cm$^3$ min$^{-1}$, whereas dry $N_2$ was introduced from the back of the balance system at 50 cm$^3$ min$^{-1}$ and sent toward the reaction tube. Both gases were exhausted through a vent at the contact part of the balance system and reaction tube. The temperature and relative humidity of the $N_2$–$H_2O$ mixed gas were continuously measured in the anterior chamber during TG–DTA measurement to calculate the $p(H_2O)$ value. Prior to the TG–DTA measurements under $N_2$–$H_2O$ gas, the instrument was calibrated with regard to the measured temperature and mass change using the same procedures applied to the DTG60 instrument but under $N_2$–$H_2O$ mixed gas with $p(H_2O)$ = ~4.5 kPa ($q_v$ = 200 cm$^3$ min$^{-1}$). For the TG–DTA measurements, an empty Pt pan (diameter: 5 mm; depth: 2.5 mm) was used as the reference for DTA and counter-balance for TG.

## S3. Thermal dehydration behavior

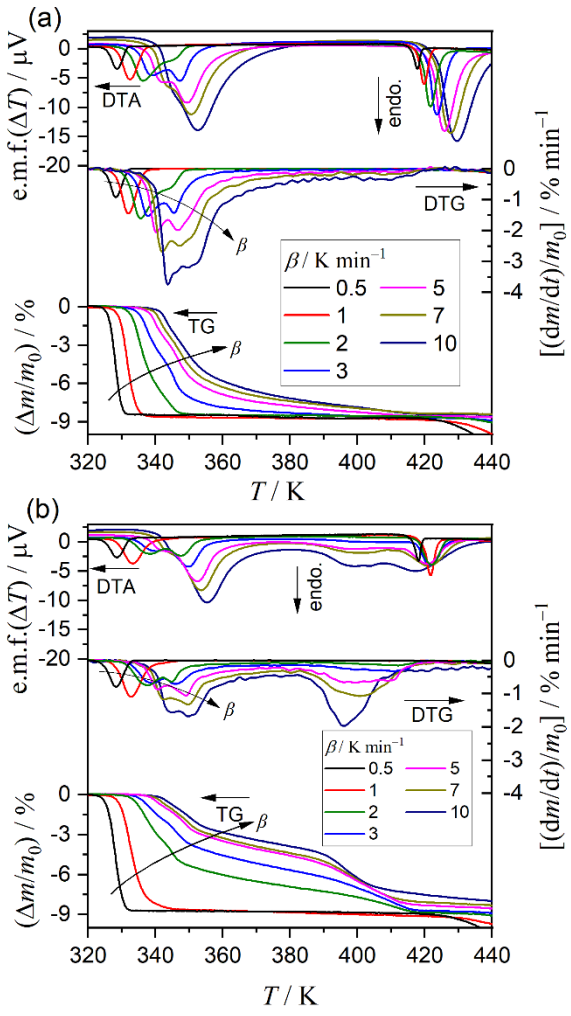


**Figure S4.** TG–DTG–DTA curves for the thermal dehydration of DG-MH under linear nonisothermal conditions at different $\beta$ values under dry $N_2$ gas ($q_v$ = 100 cm$^3$ min$^{-1}$): (a) 90–150 μm sample ($m_0$ = 5.01 ± 0.03 mg) and (b) 300–500 μm sample ($m_0$ = 5.01 ± 0.02 mg).

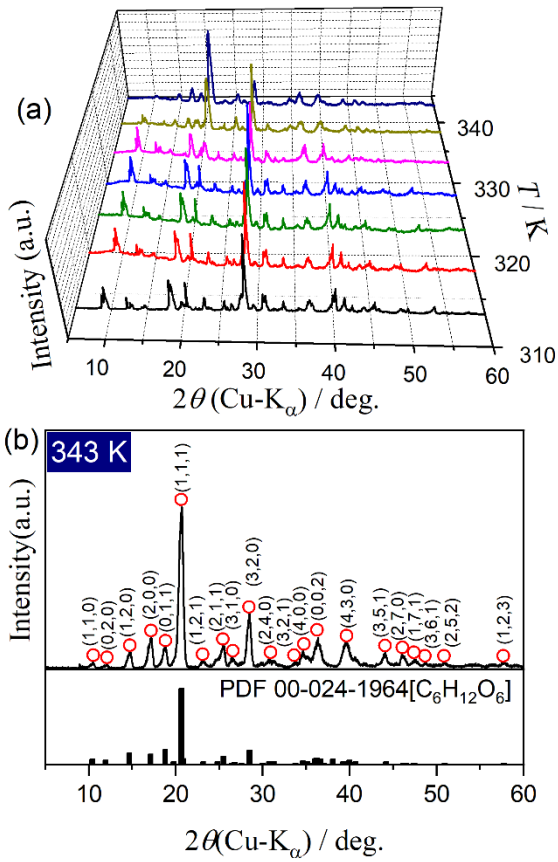


**Figure S5.** Changes in the XRD pattern of the sample during heating via the stepwise isothermal mode from 313 to 343 K at a $\beta$ of 1 K min$^{-1}$ with the 15 min isothermal holding sections at each 5 K under dry $N_2$ gas ($q_v$ = 100 cm$^3$ min$^{-1}$): (a) XRD patterns at different temperatures and (b) at 343 K.

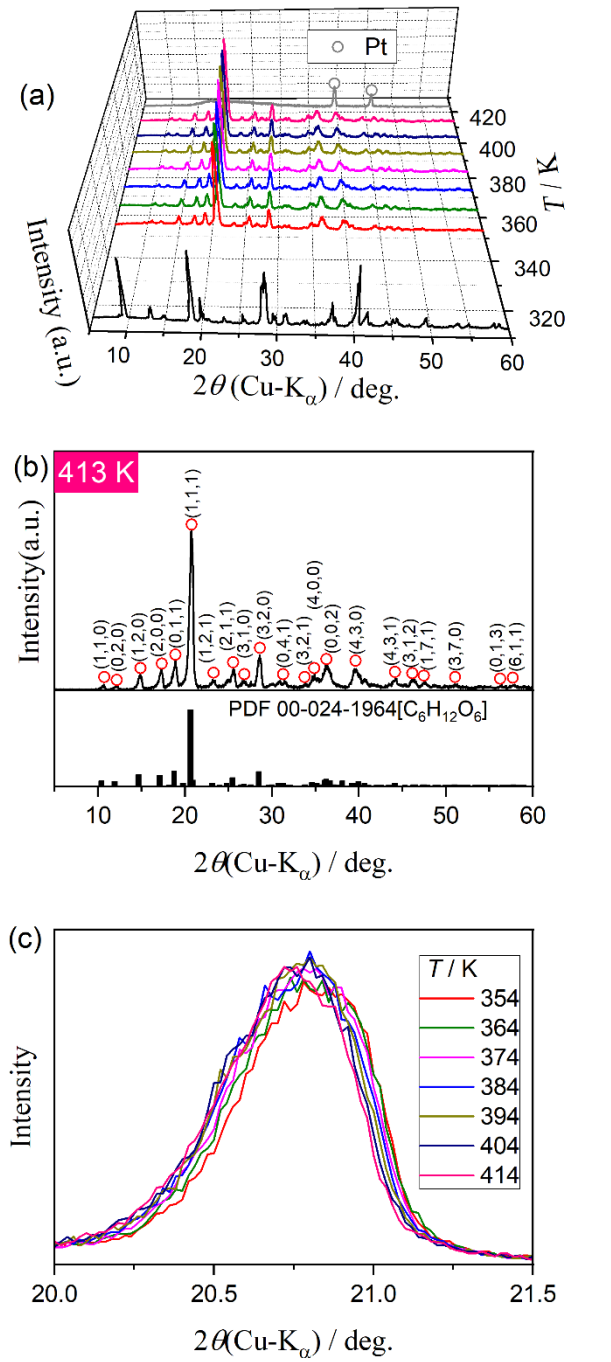


**Figure S6.** Changes in the XRD pattern of the sample heated initially from 313 to 343 K at a $\beta$ of 10 K min$^{-1}$ and subsequently from 343 to 423 K at a $\beta$ of 2 K min$^{-1}$ with the 15 min isothermal holding sections at each 10 K under dry $N_2$ gas ($q_v$ = 100 cm$^3$ min$^{-1}$): (a) XRD patterns at different temperatures, (b) at 413 K, and (c) comparison of intensity of (1, 1, 1) peaks at different temperatures.

## S4. Melting of DG-MH and anhydride

The thermal dehydration and melting of DG-MH and the melting of DG-anhydride were traced using differential scanning calorimetry (DSC; DSC120, Seiko Instrument) to the determine individual transformation temperatures and enthalpy changes ($\Delta H$). Approximately 10.0 mg of the sample particles (300–500 μm) was weighed in an Al cell (diameter: 6 mm; height: 8 mm; capacity: 70 μL) and hermetically sealed with an Al lid (withstanding pressure: 3 MPa). The hermetically sealed Al cell was heated from 293 K to 373 K at $\beta$ = 5 K min$^{-1}$ in a stream of dry $N_2$ ($q_v$ = 100 cm$^3$ min$^{-1}$) to facilitate recording of the DSC endothermic peak of DG-MH melting. The mass of the hermetically sealed cell was measured before and after the DSC run to confirm no detectable mass change. Similarly, approximately 11.5 mg of the sample particles (300–500 μm) was weighed in the Al cell. The DSC curves for the sample weighed in the open cell was recorded by heating from 293 K to 373 K at $\beta$ = 0.2 K min$^{-1}$ in a stream of dry $N_2$ ($q_v$ = 50 cm$^3$ min$^{-1}$) to facilitate measuring of the endothermic DSC peak for the thermal dehydration of DG-MH. The change in the total mass of the Al cell with the sample before and after the DSC measurement was recorded to determine the mass of the dehydration product (DG-anhydride). Thereafter, the Al cell containing the dehydration product was hermetically sealed using an Al lid. The hermetically sealed Al cell containing DG-anhydride (approximately 10.4 mg) was heated from 293 K to 450 K at $\beta$ = 5 K min$^{-1}$ to facilitate recording of the DSC curve of the melting of the anhydride. The mass of the hermetically sealed Al pan was measured before and after the DSC run to confirm no detectable mass change. The individual DSC runs were repeated four times. It is acknowledged that the temperature and energy calibrations of the DSC instrument were performed preliminary with reference to the melting point and enthalpy change of melting of pure metals (Ga and In, >99.99% purity, Nilaco). The pure metal samples were weighed in the Al cell and hermetically sealed. The DSC peaks for the melting of individual pure metals were recorded at $\beta$ = 5 K min$^{-1}$ in a stream of dry $N_2$ ($q_v$ = 50 cm$^3$ min$^{-1}$).

Figure S7 shows typical DSC curves for the thermal dehydration and melting of DG-MH, as well as the melting of DG-anhydride. The individual DSC runs were repeated four times. Table S2 lists the experimentally determined transformation temperatures and enthalpy changes.

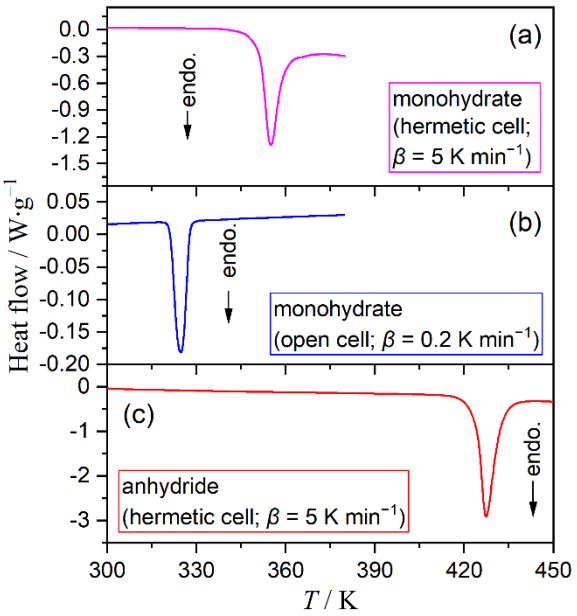


**Figure S7**. Typical DSC curves for DG-MH and DG-anhydride: (a) melting of DG-MH ($m_0$ = 10.00 mg in a hermetic cell) at $\beta$ = 5 K min$^{-1}$; (b) thermal dehydration of DG-MH ($m_0$ = 11.55 mg in an open cell) at $\beta$ = 0.2 K min$^{-1}$ under dry $N_2$; and (c) melting of DG-anhydride ($m_0$ = 10.45 mg in a hermetic cell) at $\beta$ = 5 K min$^{-1}$.

**Table S2**. Results of DSC measurements for DG-MH and DG-anhydride samples ($N$ = 4)

| Sample | Cell | $\beta$ / K min$^{-1}$ | Transformation | $T_{eo}$ / K | $\Delta H$ / J g$^{-1}$ |
|---|---|---|---|---|---|
| **DG-MH** | hermetic | 5 | fusion | 350.9 ± 0.3 | 89.9 ± 0.7 |
| **DG-MH** | open | 0.2 | dehydration | 320.3 ± 0.1 | 267 ± 4 |
| **DG-anhydride** | hermetic | 5 | fusion | 424.1 ± 0.4 | 202 ± 4 |

## S5. Kinetics of the thermal dehydration in the solid state

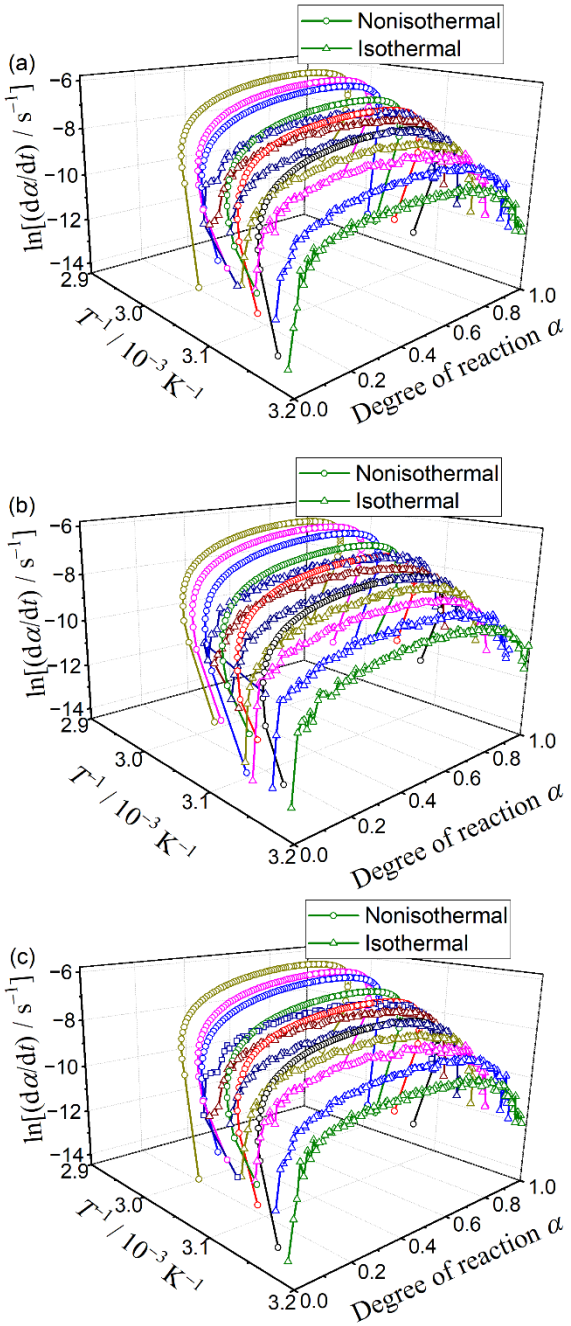


**Figure S8**. 3D-representation of the kinetic curves for the solid-state thermal dehydration of DG-MH samples of different particle sizes: (a) 90–150 μm, (b) 150–300 μm, and (c) 300–500 μm.

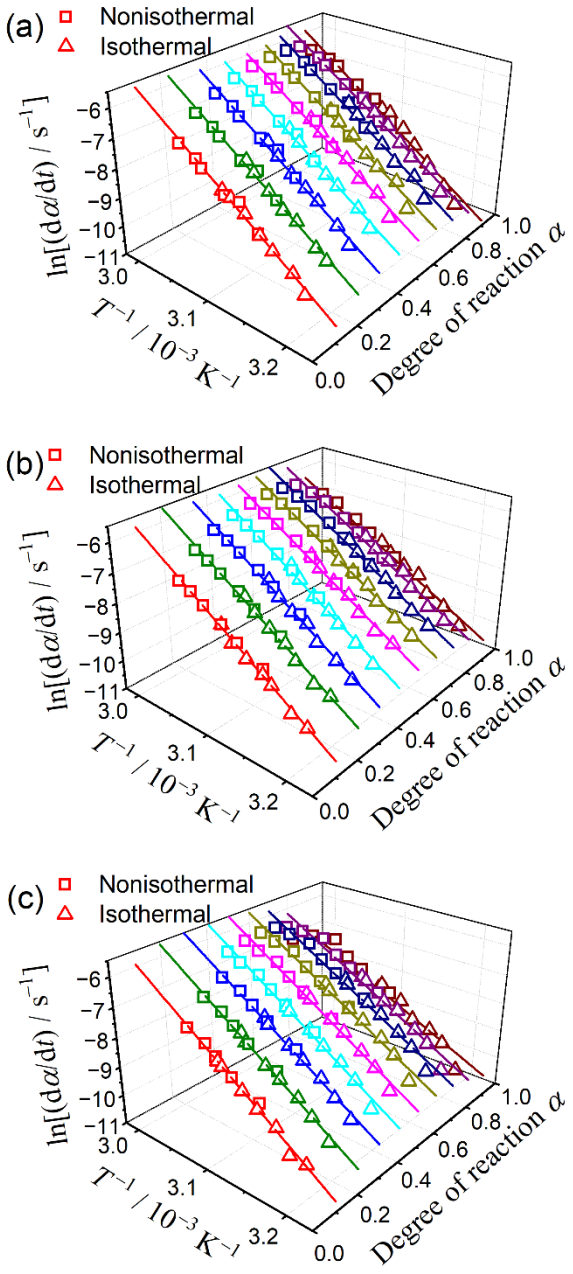


**Figure S9**. Friedman plots at various $\alpha$ values for the solid-state thermal dehydration of DG-MH samples of different particle sizes: (a) 90–150 μm, (b) 150–300 μm, and (c) 300–500 μm.

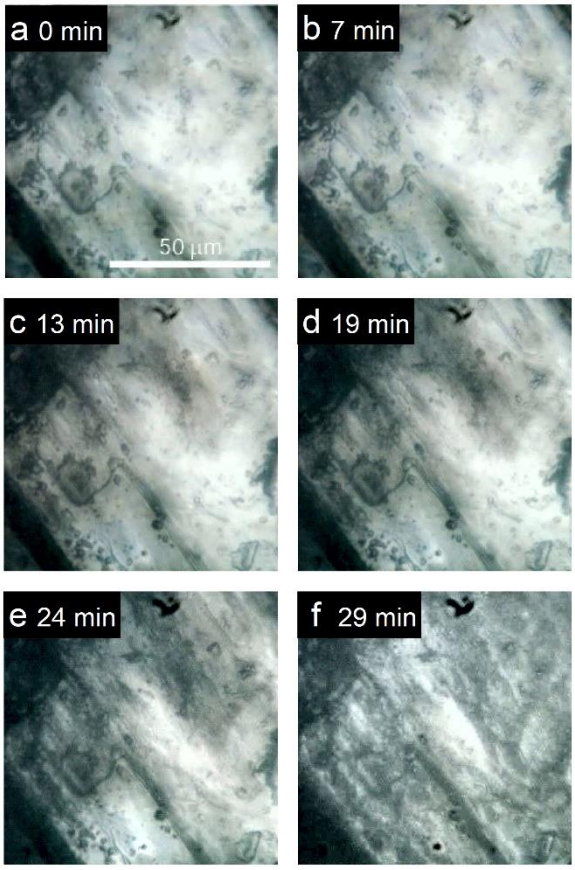


**Figure S10.** Changes in the surface morphology of a selected DG-MH particle (300–500 µm) during heating at 322 K for different times: (a) 0 min, (b) 7 min, (c) 13 min, (d) 19 min, (e) 24 min, and (f) 29 min.

**Table S3.** Contributions ($c_i$) of component steps $i$ determined by MDA for the four-step thermal dehydration of DG-MH

| Particle size/µm | $\beta$ / K min$^{-1}$ | $c_1$ | $c_2$ | $c_3$ | $c_4$ | $R^{2,a}$ |
|---|---|---|---|---|---|---|
| **90–150** | 2 | 0.69 | 0.24 | 0.06 | --- | 0.9896 |
| | 3 | 0.46 | 0.39 | 0.12 | 0.04 | 0.9921 |
| | 5 | 0.34 | 0.50 | 0.10 | 0.06 | 0.9893 |
| | 7 | 0.32 | 0.46 | 0.16 | 0.05 | 0.9957 |
| | 10 | 0.31 | 0.41 | 0.17 | 0.12 | 0.9960 |
| **150–300** | 2 | 0.52 | 0.29 | 0.18 | 0.02 | 0.9928 |
| | 3 | 0.29 | 0.33 | 0.25 | 0.12 | 0.9940 |
| | 5 | 0.21 | 0.39 | 0.22 | 0.19 | 0.9880 |
| | 7 | 0.22 | 0.32 | 0.21 | 0.26 | 0.9966 |
| | 10 | 0.22 | 0.30 | 0.19 | 0.28 | 0.9925 |
| **300–500** | 2 | 0.36 | 0.23 | 0.26 | 0.15 | 0.9934 |
| | 3 | 0.19 | 0.31 | 0.21 | 0.30 | 0.9925 |
| | 5 | 0.14 | 0.24 | 0.26 | 0.36 | 0.9873 |

[a]Determination coefficient of the least-squares analysis.